Electrochimica Acta 221 (2016) 177–183

Contents lists available at ScienceDirect

Electrochimica Acta

journal homepage: www.elsevier.com/locate/electacta

The decisive role of electrolyte concentration in the performance of aqueous chloride-based carbon/carbon supercapacitors with extended voltage window

Edurne Redondo, Eider Goikolea*, Roman Mysyk

CICenergiGUNE, Arabako Teknologi Parkea, Albert Einstein 48, 0150 Miñano, Spain

ARTICLE INFO

Article history:
Received 4 August 2016
Received in revised form 28 September 2016
Accepted 21 October 2016
Available online 22 October 2016

Keywords:
Supercapacitors
microporosity
activated carbon
neutral aqueous electrolytes
chlorides

ABSTRACT

In the present study aqueous alkali metal chloride electrolytes are investigated as potential candidates for carbon/carbon supercapacitors. High-current capacitance retention is greatly enhanced by using the electrolyte concentrations at the maximum electrical conductivity, *i.e.* 6 M LiCl, 5 M NaCl and 2 M KCl, in supercapacitor cells working at 1.6 V. The resistance of the symmetric cells is also significantly diminished by using the optimum electrolyte concentrations, with remarkable improvements not only in the equivalent series resistance, but also in the distributed resistance. Both high-rate capacitance and lower resistance are beneficial to increase the energy of supercapacitors working at high discharge rates. The small size of electrosorbed dehydrated chloride ions allows the use of less expensive carbons with narrower micropores instead of strongly activated carbons with larger micropores required for bulkier anions.

1. Introduction

Electrochemical capacitors or supercapacitors have found their niche as a promising solution for fast charging and regenerative energy acquisition. In most of the applications they are used to complement batteries but, owing to their excellent low temperature performance, calendar and cycle life, fast charge-discharge and reliability [1], they can even replace them in those applications where size and weight are not of primary concern. One of the key parameters hindering the more extensive use of supercapacitors is indeed their low energy density; in the best cases about an order of magnitude lower than batteries [2]. Two main approaches can be followed to increase the energy density of supercapacitors; one involves the usage of active materials of higher capacitance and the other one the enlargement of the cell voltage by using novel electrolytes and asymmetric/hybrid cells [3]. Although several transition metal oxides and polymers have exhibited capacitance values that exceed by far those obtained with carbonaceous materials (up to 1000 F g^{-1} *vs.* 250 F g^{-1}), the latter ones continue to be the materials of choice as they provide the best trade-off between performance and cost. Linked to environmental consciousness, the exploitation of sustainable and renewable systems for the preparation of electrode materials is nowadays a priority, and thus, activated carbons (ACs) derived from biomass feed-stock or natural wastes are acquiring increased importance in the field of supercapacitors [4].

The use of aqueous over organic electrolytes has the advantage of providing lower equivalent series resistance (ESR), higher ionic conductivity, and higher capacitance. Safety is another important parameter that is strengthened when working with water instead of organic solvents such as acetonitrile or propylene carbonate [5]. For instance, acetonitrile can cause cyanide poisoning and has a flash point of only 6 °C [6] (Flammability of Chemical Substances, 2003-2004). Nevertheless, the energy stored in a supercapacitor is proportional to the square of the cell voltage as expressed in Eq. (1),

$$E = \frac{1}{2}CV^2 \quad (1)$$

where C is the capacitance and V the cell voltage. Thus, most of the commercially available supercapacitors work in organic-based electrolytes due to the limited voltage window of alkali- and acid-based aqueous systems, typically below 1 V (thermodynamic stability window of water is 1.23 V) while organic systems can easily reach 2.5–2.7 V [7,8].

Very recently several studies have shown that electrodes made of AC can work in aqueous sulphate salts in a voltage window of about 1.9 V without significant capacitance fading [9–11]. A local

* Corresponding author.
E-mail address: egoikolea@cicenergigune.com (E. Goikolea).

http://dx.doi.org/10.1016/j.electacta.2016.10.141
0013-4686/

increase in the concentration of OH^- ions in the porosity of the negative carbon electrode due to water reduction and concomitant weak chemisorption of atomic hydrogen seems to be the reason for the extended voltage window [11], shifting the potential of molecular hydrogen evolution at the negative electrode to lower values (according to the Nernst equation) [12]. All these results have opened up the possibility of using inexpensive and less hazardous electrolytes without drastically sacrificing the energy density of the device. On the electrode side, the compatibility between the size of ions and pores should be sought at least to maximize volumetric capacitance. Additionally, some studies claim that areal capacitance can be enhanced if the pore size and ion size are matched [13–15]. However, for an efficient power response, the ion size should be slightly smaller than the carbon pore size [16]. Monovalent anions such as Cl^- are electrosorbed in the nonhydrated state whereas sulphate ions are adsorbed in the hydrated state with a size exceeding 0.733 nm [9]. In this sense, if smaller ions such as Cl^- (a diameter slightly larger than 0.362 nm [13]) could also be successfully used in an extended-voltage cell instead of a much bulkier sulphate anion, a larger variety of ultramicroporous carbon electrodes with moderate specific surface area (SSA) could be employed. Importantly, such carbons can be expected to be somewhat denser (because of their moderate pore volume) and less expensive (milder activation conditions). However, the main problem caused by the presence of chlorides is pitting corrosion occurring on several metals, which reduces the choice of well-suited current collectors. To conclude, the affordability and variety of compatible carbons make chlorides an alternative to other neutral salts, provided inexpensive chloride-resistant current collectors are used.

This work concentrates on the enhancement of chloride-based aqueous symmetric supercapacitors through the optimization of electrolyte concentration using two microporous carbons with significantly different pore size distributions.

2. Experimental

2.1. Preparation of microporous carbons by alkali activation

The activation of carbons was conducted after carbonization of raw olive pits as described elsewhere [17]. Briefly, the raw material was heated under an Ar flow of 100 ml min^{-1} at a ramp rate of 5 °C min^{-1} in a tubular furnace to a predefined temperature and further holding the temperature for 2 h at 700 °C (the carbonization yield for olive pits is 25 ± 1%). After carbonization, the resulting char was physically mixed with potassium hydroxide, KOH, in a mass ratio of 1 to 6 and 1 to 2. The materials mixed with KOH were placed in an Inconel© boat and activated by heating up to 700 °C under Ar flow (100 ml min^{-1}) inside a horizontal stainless steel tube within a tubular furnace. The heating ramp rate was 5 °C min^{-1} and the holding time at 700 °C was 2 h. After activation, the resulting microporous carbons, hereafter referred to as AC16 and AC12 (see Table S1), were washed off with a diluted solution of hydrochloric acid and water until neutral pH was reached and then dried at 120 °C under vacuum. The activation yield was 65 % and 75 %, correspondingly.

2.2. Textural and X-ray photoelectron spectroscopy characterization

Nitrogen adsorption isotherms were measured at −195.8 °C using a Micromeritics ASAP 2020 instrument for relative pressure (P/P_0) between 10^{-8} and 0.995 for samples preliminarily outgassed for 24 h at 200 °C. The SSA values and pore size distribution were calculated by applying the recently-developed 2D Non Local Density Functional Theory (2D NLDFT) treatment to N_2 adsorption isotherms using the data reduction software SAEIUS [18]. The average pore size (L_0) was calculated as a weighted average from the DFT data according to the formula:

$$L_0 = \frac{\int_{V\min}^{V\max} L dV}{V_{\max} - V_{\min}} \quad (2)$$

where V_{max} and V_{min} are the total pore volume and the pore volume at the minimum pore size, correspondingly, and L the pore size corresponding to the total pore volume V accumulated by the pores with size $\leq L$.

XPS C1 s and O1 s spectra were recorded using PHOIBOS 150 analyser (SPECS, Germany) and monochromated Mg K_α X ray source.

2.3. Electrode preparation and electrochemical measurements

Electrodes were prepared by mixing AC (95 wt. %) and polytetrafluorethylene (PTFE) binder (5 wt. %, from a 60 wt. % aqueous dispersion, Sigma-Aldrich) with a few millilitres of ethanol until plasticity was achieved. The plastic composite was then rolled to a thickness of ~200 μm and dried under vacuum at 120 °C overnight. Electrodes of 11 mm in diameter were then cut, weighed, and their thickness was measured again. Finally, two-electrode symmetric supercapacitor cells were assembled in a Nylon Swagelok® airtight system, using two titanium current collectors, a porous glass fibre (Whatman GFB) membrane separator and Li, Na and K chloride solutions of various concentrations as supporting electrolytes. A saturated calomel electrode (SCE) was used to monitor the potential evolution of each electrode in some of the symmetric two-electrode cells.

Cyclic voltammetry (CV), galvanostatic (GA) charge-discharge cycling and electrochemical impedance spectroscopy (EIS) measurements were conducted using a multichannel VMP3 generator (Biologic, France). EIS measurements were carried out by applying a low sinusoidal amplitude alternating voltage of 10 mV at frequencies from 1 MHz to 10 mHz using the same instrument.

The average gravimetric capacitance per electrode of a two-electrode symmetric cell was calculated from the data of the GA experiments according to the formula:

$$C = 2\frac{\int Idt}{\Delta V m_{am}} \quad (3)$$

where C is the gravimetric capacitance per electrode (F g^{-1}), Idt the differential charge (A s), ΔV the cell voltage (V), m_{am} the mass of active material per electrode (g). The capacitance values are reported for the voltage range between 0 V and the maximum cell voltage, excluding the voltage drop from equivalent series and distributed resistance.

The differential gravimetric capacitance per electrode of a two-electrode cell in the CV experiments was calculated according to the formula:

$$C = \frac{2i}{\left(\frac{dV}{dt}\right) m_{am}} \quad (4)$$

where C is the gravimetric capacitance per electrode (F g^{-1}), i the instant current (A), dV/dt the scan rate (V s^{-1}), m_{am} the mass of active material per electrode (g).

Three-electrode CV measurements were conducted in Swagelok cells by scanning an activated carbon (AC12 or AC16) pellet as the working electrode *vs.* a saturated calomel electrode in 6 M LiCl, 5 M NaCl, and 2 M KCl electrolytes using an oversized Norit DLC Super 30 activated carbon as the counter electrode.

The floating test procedure applied to the cells was described previously by Kötz et al. [19]. Briefly, a maximum voltage was applied to the cells and during this voltage holding period, 5 GA charge/discharge cycles at a constant current of 1 A g^{-1} were

performed every 2 h between 0 and the maximum usable voltage so as to determine the specific capacitance.

The electrical conductivity was evaluated on pelletized electrodes using the van der Pauw four-probe method [20], measuring 2 and 30 $S.m^{-1}$ for carbons AC12 and AC16, correspondingly.

3. Results and discussion

3.1. Textural characterization of carbons

Fig. 1 depicts the pore size distribution of carbons AC12 and AC16, demonstrating that the first is almost exclusively made up of subnanometer pores whereas the second exhibits a broad micropore size distribution with almost no mesoporosity. The values of L_0 for AC12 and AC16 are 0.65 nm and 1.15 nm, correspondingly, suggesting that there should be no restrictions for either alkali cations or chloride anions (an electrosorbed size of 0.362-0.421 nm [13]) although the accessibility of sulphate ions would be limited for AC12 carbon (0.58-0.733 nm [9]). Remarkably, the L_0 value of the moderately activated carbon AC12 exceeds the size of sulphate ions only marginally, implying that the comparison of supercapacitors based on chloride and sulphate-based electrolytes can reveal differences in performance connected with the effect of pore size.

More precisely, the 2D NLDFT data allow calculating the average effective pore size accessible to any specific ion [17], which can be defined as:

$$L_{0e} = \frac{\int_{V_e}^{V\max} LdV}{V_{\max} - V_e} \quad (5)$$

where L_{0e} is the effective average accessible pore size; V_{max} is the total pore volume; and V_e is the volume pertaining to pores smaller than ion diameter.

Knowing the diameter of the electrosorbed ions (as discussed above), it is easy to see from Fig. 1 that L_{0e} coincides with L_0 for alkali and chloride ions (no pores below the ion sizes are probed by N_2) whereas L_{0e} and L_0 for sulphate ions are calculated to be slightly different, 0.79 nm *vs.* 0.65 nm for AC12 and 1.24 nm *vs* 1.15 nm for AC16, correspondingly. Textural properties of both carbons are summarized in Table S1.

3.2. Electrochemical characterization

In order to investigate the best alternatives to aqueous neutral sulphate electrolytes and to remove possible restrictions of the electrolyte ions accessing the pores, a screening of various salts was undertaken using AC16 carbon with a relatively broad pore size distribution. Two-electrode symmetric cells were prepared and CVs were recorded in the safe voltage range of 0 to 1.0 V. Based on previous results where a better ion-mobility of Li^+ was evidenced over that of Na^+ and K^+ [9], in all cases Li^+ was selected as the common cation. Fig. 2 shows the CVs recorded using 1 M lithium sulphate, nitrate and chloride at 5 mV s^{-1}. All the CVs in Fig. 2 approach the typical rectangular shape of supercapacitors. Moreover, the results show that regardless of the nature of the anion, the electrochemical performance of all cells is very similar, with the capacitance values ranging from 87 F g^{-1} for 1 M Li_2SO_4 to 111 F g^{-1} for 1 M LiCl. The slightly higher values for LiCl and $LiNO_3$ can be ascribed to the smaller size of monovalent NO_3^- and Cl^- ions (0.36 nm) in an electrosorbed nonhydrated state as compared to hydrated bivalent SO_4^{2-} ions (> 0.58 nm) [13]. Therefore, it can be speculated that this allows monovalent nonhydrated ions to access a larger portion of SSA, encompassing a higher volume of narrower pores, giving rise to a higher gravimetric capacitance. In what follows we chose to optimize chloride electrolytes because the preliminary evaluation had shown high capacitance decay for nitrate based electrolytes if the cell voltage is set to above 1 V (Fig. S1).

In order to optimize the cell performance, especially at high current densities, we studied the effect of electrolyte concentration. It is well known that 6 M KOH and 1 M H_2SO_4 have the highest conductivity values among the commonly employed aqueous electrolytes, 625 and 425 mS cm^{-1}, respectively, at 25 °C [21,22]. In the case of neutral chloride electrolytes, the maximum electrical conductivities are obtained when the concentrations are 6 M LiCl (170 mS cm^{-1}), 5 M NaCl (220 mS cm^{-1}) and 2 M KCl (205 mS cm^{-1}) (Fig. S2) [21]. Fig. 3 shows the CVs obtained at 5 mV s^{-1} using 1 M and the above mentioned concentrations (at 1 V). In all cases, increasing the concentration is beneficial for the cell performance, leading to almost perfectly rectangular-shaped CVs with a nearly negligible resistive contribution. Additionally, the capacitance values are identical for all systems, viz. ~150 F g^{-1}, and the CV curves can be perfectly superimposed one on top of the other for the concentrations providing the maximum electrolyte conductivity. Thus, as distinct from sulphate-based supercapacitors where the maximum electrolyte conductivity did not provide the highest capacitance and the lowest resistance [9], the optimum cell response follows the maximum electrolyte conductivity in the case of chlorides.

Electrochemical impedance spectroscopy is another technique that can help in assessing the differences derived from the use of different electrolytic solutions. All the cells in Fig. 4 exhibit the typical supercapacitor impedance behaviour, characterized by a near-vertical low-frequency line changing into a steep medium-frequency line intersecting the real axis with a ~45° angle. The

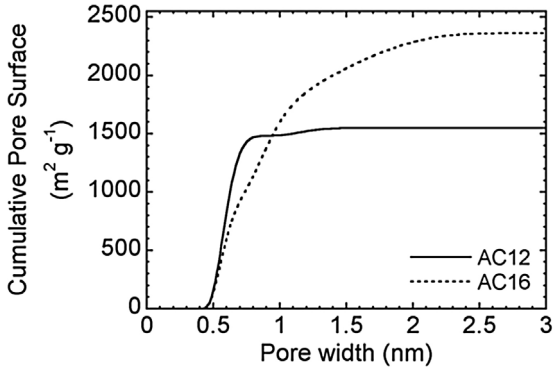

Fig. 1. Pore size distribution of carbons AC12 and AC16.

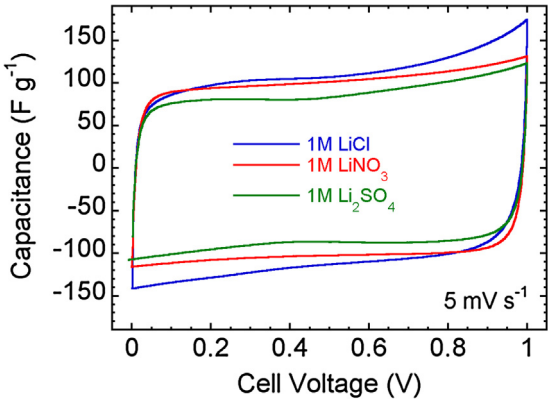

Fig. 2. Cyclic voltammogramms of symmetric supercapacitors using carbon AC16 and various inorganic lithium salts.

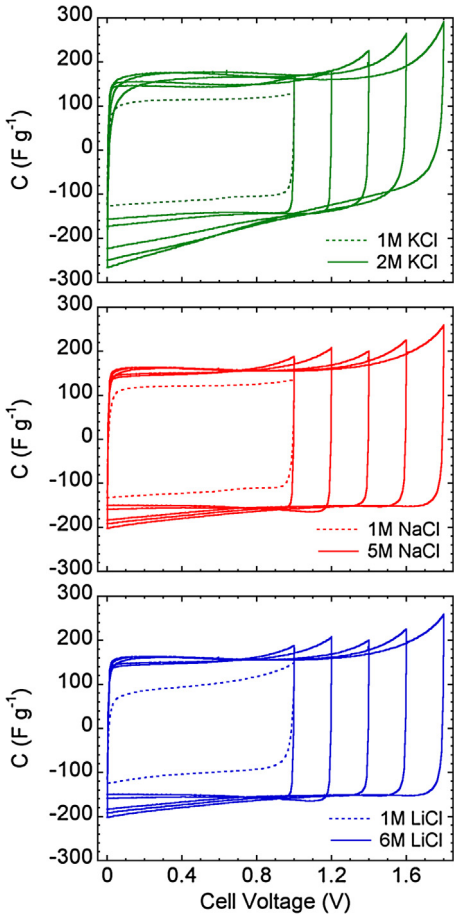

Fig. 3. CVs of symmetric supercapacitor cells (at 5 mV s^{-1}) using carbon AC16 in 1 M chloride solutions and 2 M KCl, 5 M NaCl and 6 M LiCl electrolytes, respectively.

intersection point (the high frequency limit) is the equivalent series resistance (ESR) which is commonly attributed to the electronic resistance of electrodes and the ionic resistance of bulk electrolyte [8]. Although in all cases the values are below ~0.50 Ω cm^2, there is a clear improvement from increasing the electrolyte concentration, reaching ESR values as low as ~0.20 Ω cm^2 in all the systems. As the electrochemical cells are prepared using the same cell components and following the same cell assembly procedure, the improvement in the ESR is assumed to be due to the higher electrolyte conductivity. Note also that the conductivities of all the electrolytes are very similar, and thus, not much divergence in the values can be expected. Moreover, for the highest electrolyte concentrations, the medium-frequency steep line, which is characteristic of ion transport in the porosity [23,24] is shifted towards lower resistance values. Noteworthy, the electrolyte resistance inside the pores is in line with the trend in the electrolyte conductivities for bulk electrolyte, which can be anticipated but is not an obvious result. As the only difference between the cells is the electrolyte concentration, it can be speculated that the lower in-pore resistance is due to the higher population of ions in the pore network, which shortens transport pathways under electrode polarization.

As is the case for their sulphate counterparts, the pH of aqueous alkali metal chloride solutions is also close to neutral, *i.e.*, the operational voltage window of the cells using these electrolytes can also be extended beyond the typical ~1.0 V of aqueous cells. Fig. 3 depicts a CV recorded for the 3 electrolytes at 5 mV s^{-1} from 1.0 V up to 1.8 V. For the cells prepared using LiCl and NaCl the shape of the CVs remains rectangular despite the increase in the cell voltage. However, the cell working in 2 M KCl exhibits a much more distorted rectangular shape, which is mostly due to water reduction (as detailed below). In fact, in the latter case the absolute value of both anodic and cathodic currents increases significantly when the cell is cycled above 1.6 V.

The lower electrolyte stability is also reflected in the rate capability (Fig. 5). The recorded capacitance at low current densities is higher in those cells using NaCl and KCl, mainly due to the faradic contribution derived from the partial electrolyte decomposition, which is not a reversible charge storage mechanism. Nevertheless, the capacitance retention is higher in the cells operating in LiCl upon increasing the current density, *i.e.* 63, 47 and 32% at 30 A g^{-1} for Li, Na and K metal chloride salts respectively.

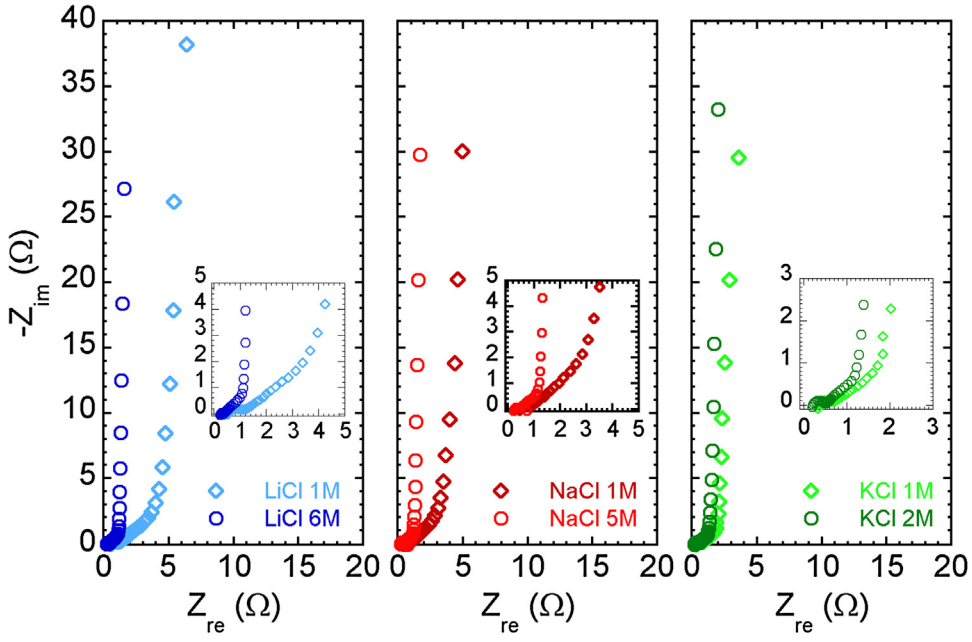

Fig. 4. Comparison of Nyquist plots for chloride-based symmetric supercapacitor cells using 1 M solutions and solutions providing maximum electrical conductivity.

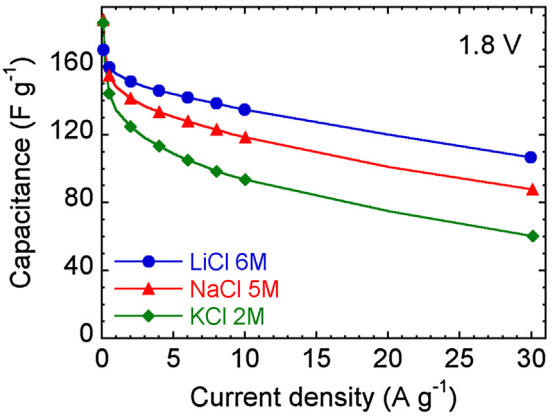

Fig. 5. Capacitance as a function of the current density for a cell voltage of 1.8 V.

In order to check the stability of the different cells at 1.8 V, floating tests were carried out. Given a certain upper cut-off voltage value, the total time required to provide for reliable stability estimation is significantly shortened in floating tests, typically taking few hundred hours over a few thousand hours spent in conventional cycling typical of battery testing. The floating tests show a clear difference among the three different systems. KCl-based cell presents a capacitance decrease of more than 50% at 1.8 V after the floating time slightly exceeding 4 h. In the case of NaCl, the capacitance decreases to 60% after a 100 h test at the same operation voltage whereas the capacitance retention is higher than 60% under the same conditions when using LiCl electrolyte (Fig. 6a). In any case, if the end-of-life criterion is set as a capacitance loss of 20% of the initial value [19], none of the symmetric systems would meet this condition if the maximum voltage is pushed up to 1.8 V.

On the contrary, when the upper cut-off voltage is decreased to 1.6 V, the cell working in 6 M LiCl exhibits a much more stable profile, retaining 80 % of the initial capacitance after holding the maximum voltage for 100 h (Fig. 6b). Thus, although the rate capability measurements suggest a voltage of 1.8 V as the optimum value, floating experiments clearly show that this upper voltage limit is too demanding. Therefore, for alkali metal chloride salts, *viz.* 6 M LiCl, 1.6 V should be considered as the optimum voltage for symmetric cells [25], which is still 0.6–0.8 V higher than the typical 0.8–1.0 V used when operating in either 6 M KOH or 1 M H_2SO_4. Although the specific capacitance of carbon AC16 in 6 M LiCl is about 45% lower than in basic or acidic media, according to Eq. (1) the specific energy of the system will still be up to 40% higher in neutral medium using chloride salts.

The reasons for the varied stability of symmetric supercapacitors based on different chloride salts can be looked into in the behaviour of the separate electrodes in two-electrode symmetric cells, as presented in Fig. 7 for cut-off voltages of 1.6 and 1.8 V. Both negative and positive electrodes work outside the thermodynamic stability window of water defined by the Nernst equation for all symmetric cells charged up to 1.8 V. However, three-electrode measurements clearly demonstrate that the practical stability range at negative potential values goes well beyond the corresponding thermodynamic stability limit. As mentioned in the introduction, this is due to the excess of OH^- ions in the porosity of the negative electrode at pH values ~7 [11,26]. By comparing the potential ranges of each electrode with the stability range defined by three-electrode measurements, one can evidence that negative electrodes operate at a potential lower than the practical potential of molecular hydrogen evolution. Noteworthy, the positive electrodes of the cells using LiCl and KCl surpass the positive potential stability limit to a lower extent

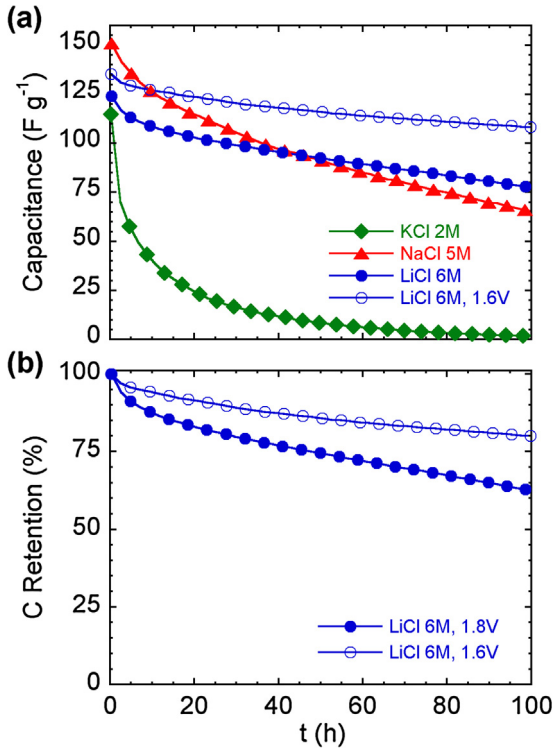

Fig. 6. Capacitance as a function of floating time: a) for chloride salts at the maximum cell voltage of 1.8 V and b) lithium chloride salts at the maximum cell voltage of 1.6 V and 1.8 V.

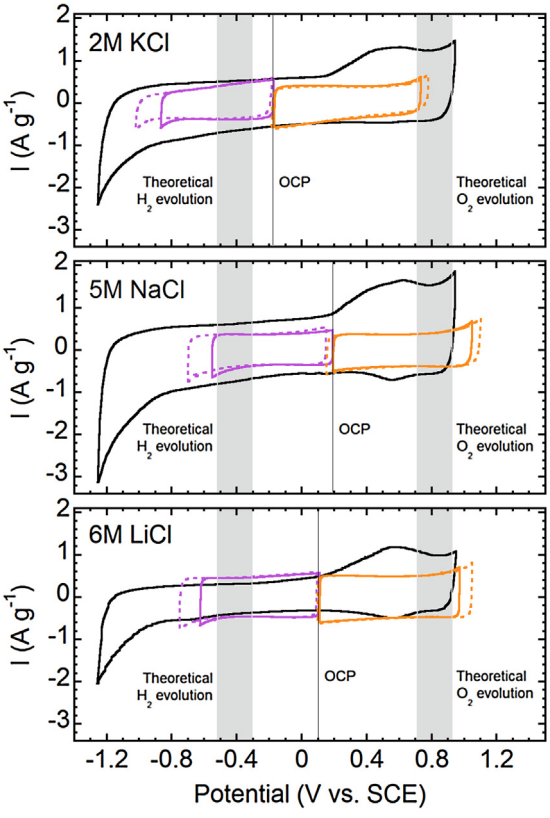

Fig. 7. Cyclic voltammograms in three- (black line) and two-electrode (positive electrode in orange and negative electrode in purple) cell configurations at 5 mV s^{-1} in 2 M KCl, 5 M NaCl and 6 M LiCl.

(virtually not exceeding the oxygen evolution potential for the cells operating up to 1.6 V) whereas the potential of the positive electrode of the NaCl-based cell is significantly above the oxygen evolution potential, which explains its worse cell performance under floating (Fig. 6a). The limitation of symmetric cells set by the positive electrode coincides with the results obtained for neutral sulphate electrolytes [26]. Fig. 7 also shows that the open circuit potential (OCP) of the cell using 2 M KCl is shifted towards more negative values compared to LiCl and NaCl-based cells. This leads to the negative electrode of the symmetric cell being close to the stability limit established from three-electrode measurements. Thus, the most probable origin of the extremely poor floating response of the 2 M KCl-based cell is dihydrogen evolution in the negative electrode. To sum up, the comparison between the CVs of three- and two-electrode cells clearly shows that a symmetric configuration is not the optimum option for neutral chloride electrolytes. Taking into account the potential of oxygen evolution and the practical potential of irreversible molecular hydrogen evolution, an asymmetric cell operating stably in a voltage window of 1.8 V can be foreseen. Further improvements can also be expected from a purposeful oxidation of carbon surface to raise the practical stability limit at the positive electrode [11].

The advantage of using an electrolytic salt with low-sized ions is further highlighted using a moderately-activated AC with most of the pores in the ultramicropore range (<0.7–0.8 nm). The advantages of such carbons can be, in some cases, their higher density (*i.e.*, higher volumetric energy) and lower cost (they are produced under milder activation conditions). For this purpose, an activated carbon prepared with a low KOH consumption in the synthesis, AC12, was selected as the active material (Table S1). For comparison with chlorides, 1 M Li_2SO_4 was chosen as the electrolyte since this concentration was shown to provide the optimum supercapacitor performance [9]. On cycling up to 1.6 V at low scan rates in both LiCl and Li_2SO_4, *i.e.* at 5 mV s^{-1}, the shape of the CVs is close to the expected rectangular profile of capacitive systems and the capacitance is similar (Fig. 8a), ~150 F g^{-1}. This is further corroborated by GA charge/discharge cycles at low current densities (Fig. 8b) (see also charge/discharge profiles in Fig. S3). However, the increase in the current density up to 30 A g^{-1} leads to a more pronounced capacitance decay in the cell working in Li_2SO_4, observing just 15% of capacitance retention for the sulphate-based cell whereas the retention of the cell working in the chloride salt is 27%. For comparative purposes the rate capability of the cell operating in 6 M LiCl is also shown, *i. e.* ~66% of capacitance retention. Again, the drastic change in capacitance retention underlines the decisive role of electrolyte concentration in ensuring efficient high-rate capacitive response.

The overall capacitance decay of the latter system is comparable to that observed when working up to 1.8 V in carbon AC16 (Fig. 5). The capacitance loss at 1.8 V for AC16 carbon with more open porosity is related to a detrimental Faradaic contribution (electrolyte decomposition in the positive electrode) whereas the capacitance loss observed for AC12 carbon at a cell voltage of 1.6 V is rather associated with the size match between the ions and the pores, impeding high-rate ion transport in the pores of AC12 to a higher extent than for AC16.

In other words, taking into account that the average pore size of AC12 is only slightly larger than the size of hydrated SO_4^{2-} (0.79 nm *vs* 0.733 nm), applying medium-to-high current density values would lead to the transport of sulphate ions being much more hindered than that of smaller Cl^- anions. Thus, these results reveal LiCl as a good alternative electrolyte choice if one aims at not being limited by the AC used as the active material in terms of pore size distribution. Despite the quite different electrical conductivities of AC12 and AC16 carbons, 2 and 30 S m^{-1} correspondingly, the capacitance retention in 6 M LiCl is very similar in both cases,

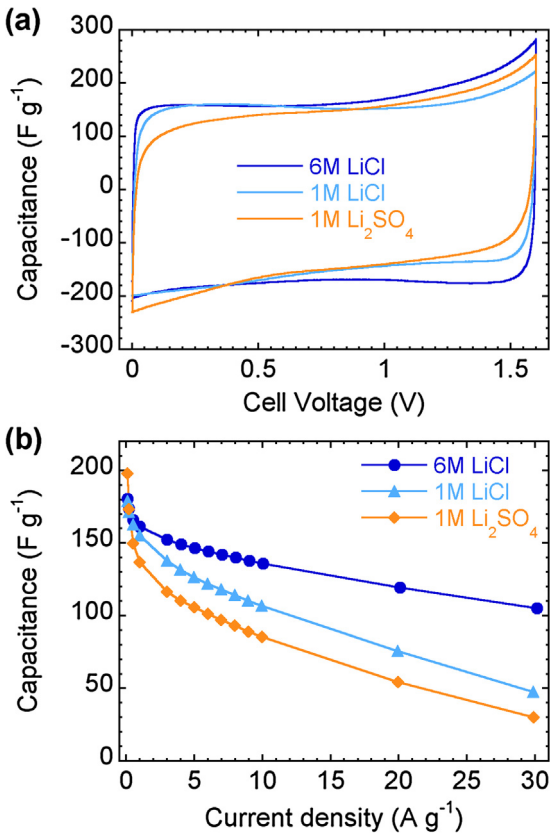

Fig. 8. (a) CVs of symmetric supercapacitor cells using AC12 carbon in LiCl and Li_2SO_4 electrolytes at 5 mV s^{-1} in a cell voltage of 1.6 V. (b) Capacitance as a function of current density for cell voltage of 1.8 V.

which also evidences that high-rate capacitance can be related to the concentration-dependent electrical conductivity of the electrolyte and not to that of the electrode material as long as carbon pores are sufficiently wide not to impede ion transport.

4. Conclusion

We have demonstrated a drastic effect of chloride salts' concentration on the performance of the corresponding symmetric supercapacitor cells: the highest capacitance retention and the lowest cell resistance are enabled by the electrolyte concentration providing the maximum electrical conductivity of the related solutions. The EIS study has clearly evidenced that bulk electrolyte conductivity not only impacts ESR, but it also significantly reduces the resistance related to the ion transport inside the pores. Knowing that chlorides can be coupled with more affordable ultramicroporous carbons due to their smaller size, we have demonstrated that using chlorides with such ultramicroporous carbons can provide better rate response in aqueous extended-voltage supercapacitors. In a broader context, our work emphasizes that optimizing electrolytes can bring about substantial improvements in the performance of supercapacitors even using traditional electrode materials such as activated microporous carbons.

Acknowledgments

The work was supported by the Basque Government under the Etortek Energigune'12 and Elkartek 2015 Programs. The authors acknowledge Norit for providing activated carbon.

Appendix A. Supplementary data

Supplementary data associated with this article can be found, in the online version, at http://dx.doi.org/10.1016/j.electacta.2016.10.141.

References

[1] P. Simon, Y. Gogotsi, Nanostructured activated carbons from natural precursors for electrical double layer capacitors, Nat Mater. 7 (11) (2008) 845–854.
[2] F. Béguin, E. Frackowiak, Supercapacitors: Materials, Systems, and Applications, Wiley-VCH Verlag GmbH & Co KGaA, 2013.
[3] F. Béguin, V. Presser, A. Balducci, E. Frackowiak, Carbons and electrolytes for advanced supercapacitors, Adv. Mater. 26 (14) (2014) 2219–2251.
[4] L. Wei, G. Yushin, Nanostructured activated carbons from natural precursors for electrical double layer capacitors, Nano Energy 1 (4) (2012) 552–565.
[5] C. Zhong, Y. Deng, W. Hu, J. Qiao, L. Zhang, J. Zhang, A review of electrolyte materials and compositions for electrochemical supercapacitors, Chem. Soc. Rev 44 (2015) 7484–7539.
[6] http://www.sigmaaldrich.com/catalog/product/sial/271004 (last access 28/09/2016).
[7] A. Burke, Ultracapacitors: why, how, and where is the technology, J.Power Sources 91 (1) (2000) 37–50.
[8] R. Kötz, M. Carlen, Principles and applications of electrochemical capacitors, Electrochim. Acta 45 (15–16) (2000) 2483–2498.
[9] K. Fic, G. Lota, M. Meller, E. Frackowiak, Novel insight into neutral medium as electrolyte for high-voltage supercapacitors, Energy Environ Sci. 5 (2) (2012) 5842–5850.
[10] L. Demarconnay, E. Raymundo-Piñero, F. Béguin, A symmetric carbon/carbon supercapacitor operating at 1.6 V by using a neutral aqueous solution, Electrochem. Comm. 12 (10) (2010) 1275–1278.
[11] Q. Gao, L. Demarconnay, E. Raymundo-Piñero, F. Béguin, Exploring the large voltage range of carbon/carbon supercapacitors in aqueous lithium sulfate electrolyte, Energy Environ Sci. 5 (11) (2012) 9611–9617.
[12] S.-E. Chun, J. Whitacre, Investigating the role of electrolyte acidity on hydrogen uptake in mesoporous activated carbons, J. Power Sources 242 (2013) 137–140.
[13] L. Eliad, G. Salitra, A. Soffer, D. Aurbach, Ion sieving effects in the electrical double layer of porous carbon electrodes: Estimating effective ion size in electrolytic solutions, J. Phys. Chem. B 105 (29) (2001) 6880–6887.
[14] J. Chmiola, G. Yushin, Y. Gogotsi, C. Portet, P. Simon, P.L. Taberna, Anomalous increase in carbon capacitance at pore sizes less than 1 nanometer, Science 313 (5794) (2006) 1760–1763.
[15] E. Raymundo-Piñero, K. Kierzek, J. Machnikowski, F. Béguin, Relationship between the nanoporous texture of activated carbons and their capacitance properties in different electrolytes, Carbon 44 (12) (2006) 2498–2507.
[16] H. Tamai, M. Kouzu, M. Morita, H. Yasuda, Highly mesoporous carbon electrodes for electric double-layer capacitors, Electrochem. Solid State Lett. 6 (10) (2003) A214–A217.
[17] E. Redondo, J. Carretero-González, E. Goikolea, J. Ségalini, R. Mysyk, Effect of pore texture on performance of activated carbon supercapacitor electrodes derived from olive pits, Electrochim. Acta 160 (2015) 178–184.
[18] J. Jagiello, J. Oliver, 2D-NLDFT adsorption models for carbon slit-shaped pores with surface energetical heterogeneity and geometrical corrugation, Carbon 55 (2013) 70–80.
[19] D. Weingarth, A. Foelske-Schmitz, R. Kötz, Cycle versus voltage hold – Which is the better stability test for electrochemical double layer capacitors? J. Power Sources 225 (2013) 84–88.
[20] L.J. van der Pauw, A method of measuring specific resistivity and Hall Effect of discs of arbitrary shape, Philips Research Reports 13 (1958) 1–9.
[21] R. Gilliam, J. Graydon, D. Kirk, S. Thorpe, A review of specific conductivities of potassium hydroxide solutions for various concentrations and temperatures, Int. J. Hydrogen Energy 32 (3) (2007) 359–364.
[22] International Critical Tables, Vol. VI, pp. 230-258; McGraw Hill, 1929.
[23] R. de Levie, Porous Electrodes in Electrolyte Solutions, I Capacitance effects, Electrochim. Acta 8 (10) (1963) 751–780.
[24] R. de Levie, On Porous Electrodes in Electrolyte Solutions -IV, Electrochim. Acta 9 (9) (1964) 1231–1245.
[25] M.P. Bichat, E. Raymundo-Piñero, F. Béguin, High voltage supercapacitor built with seeweed carbons in neutral aqueous electrolyte, Carbon 48 (2010) 4351–4361.
[26] Q. Abbas, P. Ratajczak, P. Babuchowska, A. Le Comte, D. Bélanger, T. Brousse, F. Béguin, Strategies to improve the performance of carbon/carbon capacitors in salt aqueous electrolytes, J. Electrochem. Soc. 162 (5) (2015) A5148–A5157.